

Examining thermolysis reactions and tautomerism of 2-mercapto-5-methyl-1,3,4-thiadiazole and 2,5-dimercapto-1,3,4-thiadiazole †

2 PERKIN

Frank Hipler, Roland A. Fischer and Jens Müller*

Ruhr-Universität Bochum, Lehrstuhl für Anorganische Chemie II – Organometallics & Materials Chemistry, D-44780 Bochum, Germany. E-mail: jens.mueller@ruhr-uni-bochum.de; roland.fischer@ruhr-uni-bochum.de; Fax: +(49)-(0)234-3214174

Received (in Cambridge, UK) 21st February 2002, Accepted 21st June 2002

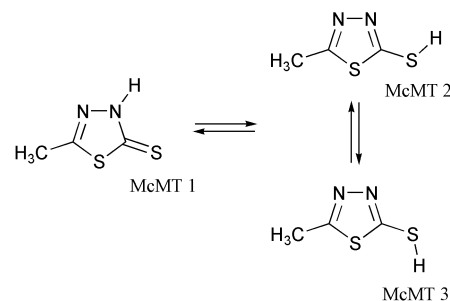
First published as an Advance Article on the web 23rd July 2002

A series of high-vacuum thermolysis experiments with 2,5-dimercapto-1,3,4-thiadiazole and 2-mercapto-5-methyl-1,3,4-thiadiazole was performed between ambient temperature and 800 °C. The thermolysis products were trapped by matrix-isolation techniques and characterised by IR spectroscopy. Thermolysis of 2,5-dimercapto-1,3,4-thiadiazole gave HNCS, CS₂ and HCN, whereas 2-mercapto-5-methyl-1,3,4-thiadiazole shows a more complex fragmentation pattern forming HNCS, CH₃NCS, HCN and CS₂. Formation of CH₃CN was not observed. The molecular structures of different isomers of both mercaptothiadiazoles were studied by *ab initio* and DFT computations.

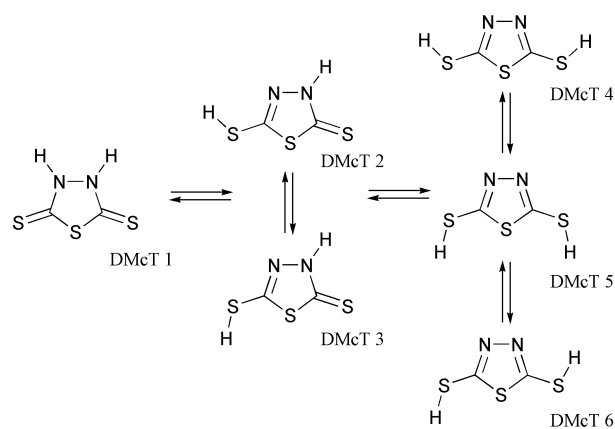
Introduction

2,5-Dimercapto-1,3,4-thiadiazole (DMcT), 2-mercapto-5-methyl-1,3,4-thiadiazole (McMT) and related compounds or derivatives have been widely studied for their applications as bioactive compounds, metal-chelating agents, lubricant additives such as corrosion inhibitors and antiwear agents, cross-linkers for polymers, and as components of cathode material battery systems.^{1–3} As in some of these applications high temperatures may occur or may even be required, it is surprising that so far no detailed investigation has been undertaken to illuminate the thermolysis behaviour of these compounds. For DMcT derivatives the decomposition pattern upon electron impact has been described,⁴ involving the formation of diazirines and carbon disulfide. However, for 1,2,3-thiadiazole and some derivatives it has been shown that thermal decomposition leads to the formation of thioketenes, R₂CCS, presumably through intermediate diazothioketenes, thioacylcarbenes or 1,3-diradicals.⁵ Pyrolysis of substituted 1,2,5-thiadiazoles has been shown to give nitrile *N*-sulfides, RCNS.⁶ With the 1,3,4-thiadiazoles possessing a different heteroatom position in the five-membered ring, we can expect a different thermolysis behaviour and fragmentation mechanism.

When discussing reaction mechanisms we have to consider one of the most interesting properties of mercapto-substituted thiadiazoles: the existence of thiol and thione tautomeric forms (Schemes 1 and 2). The tautomerisation influences the reactivity of the thiadiazoles, which has been demonstrated for polymerisation processes² and substitution reactions at the different moieties.^{1,7} In the solid state DMcT is actually present as the thione–thiol tautomer as shown by vibrational spectroscopy and X-ray structure analysis,⁸ while in solution a solvent-dependent equilibrium is believed to exist between the thione–thiol and thione–thione forms, the former being the prevailing species in polar solvents.¹ It has also been proposed that DMcT exists predominantly in the dithione form and the fact that reaction with alkyl halides in basic ethanol gives the *S*-alkylated derivatives was rationalised by the higher kinetic nucleophilicity of sulfur.⁷ An *ab initio* study (HF/STO-3G and HF/4-31G*



Scheme 1



Scheme 2

levels) of the gas-phase equilibria of DMcT predicted the thione–thiol tautomer to be the most stable,⁹ again in accordance with X-ray investigations.⁸ For McMT, spectral data indicate that the thione tautomer exists predominantly in DMSO solution as well as in the solid state.¹⁰ Before this study, structural data on the molecular structure in the solid state were not known.

The objective of our current studies is to investigate the thermolysis behaviour of mercapto-functionalised thiadiazoles. In contrast to experiments conducted in the bulk phase, applying matrix-isolation techniques enables us to observe primary reaction products and reactive species. The reaction products are rapidly trapped in an inert argon matrix, and

† Electronic supplementary information (ESI) available: calculated molecular structures in cartesian co-ordinates as well as calculated IR spectra of all McMT and DMcT isomers. See <http://www.rsc.org/suppdata/p2/b2/b201887j/>

Table 1 Gas-phase electronic energies (E_{elec}) and dipole moments (μ) of different McMT and DMcT tautomers at the B3LYP/6-311+G(d,p) level of theory

Compound	$E_{\text{elec}}/\text{au}^a$	$\Delta E_{\text{elec}}/\text{kJ mol}^{-1}$	ZPVE/ kJ mol^{-1}	μ/D^b
McMT 1	-1022.669452	0.0	193.16	4.24
McMT 2	-1022.655294	37.2	182.03	2.46
McMT 3	-1022.653643	41.5	181.71	4.26
DMcT 1	-1381.568772	24.6	125.84	3.61
DMcT 2	-1381.578154	0.0	117.53	3.70
DMcT 3	-1381.576577	4.14	117.26	3.04
DMcT 4	-1381.565498	33.2	106.79	1.32
DMcT 5	-1381.561901	42.7	106.51	4.68
DMcT 6	-1381.562866	40.1	106.21	3.12

^a 1 au = 2625.5 kJ mol⁻¹. ^b 1 D = 3.33564 × 10⁻³⁰ C m.

due to the low temperature and the fact that the molecules are highly diluted in the matrix, secondary reactions are suppressed.

Experimental

All reactions and manipulations were carried out under an argon atmosphere utilizing standard Schlenk techniques. Commercially available compounds, 2,5-dimercapto-1,3,4-thiadiazole (Lancaster, 98+%) and 2-mercapto-5-methyl-1,3,4-thiadiazole (Aldrich, 99%) were sublimed prior to use. FT-Raman spectra were measured with an FRA 106 Raman module attached to an IFS 66 FT-IR spectrometer (Bruker), and 1064 nm radiation from a Nd-YAG laser with a power of 450 mW was used for excitation.

Matrix isolation

The matrix apparatus consisted of a vacuum line and a Displex CSW 202 cryogenic closed-cycle system (APD Cryogenics Inc.) fitted with CsI windows. Compounds were kept in a small heatable metal container connected to the matrix apparatus. In a typical matrix experiment the gaseous thiadiazoles, evaporated at container temperatures of 60–100 °C and highly diluted in argon as carrier gas, were passed through an Al₂O₃ tube with two parallel inner channels [outer diameter of 4 mm; inner diameter of 1 mm each; the rear part (15 mm) heated with a tungsten wire] with one of the inner channels equipped with a thermocouple. The experiments were performed with oven temperatures in the range of ambient temperature to 800 °C. The gaseous mixtures were trapped onto the CsI window at 20 K. The IR spectra of the matrices, cooled to 10–11 K, were recorded on a Bruker EQUINOX 55 with a KBr beam splitter in the range of 400–4000 cm⁻¹ with a resolution of 1.0 cm⁻¹.

Computational methods

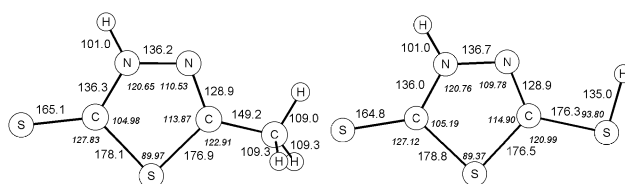
The different isomers of McMT and DMcT were subjected to geometry optimisations at various levels of theory by using the Gaussian98 package.¹¹ *Ab initio* calculations for the structures were carried out at the HF and MP2(fc) levels. DFT, in the form of Becke's three-parameter exchange functional, in combination with the Lee, Yang, and Parr correlation functional (B3LYP), was also used for geometry optimisation and for frequency calculations. In the calculations the triple ζ split valence basis set 6-311+G(d,p) was used. Calculation of the harmonic vibrational frequencies confirmed the minimum-energy geometries to be minima on the potential energy surface (no imaginary frequencies).

Results and discussion

DFT calculations of thiadiazole tautomers

The molecules were first studied by conformational analysis to

find the most stable structures in the gas phase at HF and B3LYP levels of theory. Details of the calculated geometries for McMT and DMcT are given in the electronic supplementary information (ESI). In the case of McMT 1 and DMcT 2 optimised structures are shown in Fig. 1.

**Fig. 1** Optimised geometries of McMT 1 and DMcT 2 with selected bond lengths (pm) and angles (°, italics), calculated at the B3LYP/6-311+G(d,p) level.

For 2-mercapto-5-methyl-1,3,4-thiadiazole, as Table 1 shows, we found two minima for the thiol tautomers (McMT 2, McMT 3) and one minimum for the thione form (McMT 1, Scheme 1). The results show that tautomer McMT 1 is the most stable form in the gas phase with ΔE_{elec} of 37.2 and 41.5 kJ mol⁻¹ to McMT 2 and McMT 3, respectively. Compared with experimental data,¹² the bond angles and bond lengths of McMT 1 (Fig. 1) are reproduced in acceptable agreement by the calculations.¹³

For 2,5-dimercapto-1,3,4-thiadiazole (Table 1, Scheme 2) we found two minima for the thiol–thiol tautomers DMcT 4 and DMcT 5 with C_{2v} symmetry involving a transition state (DMcT 6) with the hydrogen atoms in a *trans* position. One minimum and one transition state were found for the thiol–thione tautomers DMcT 2 and DMcT 3, respectively, and one minimum for the thione–thione form DMcT 1. The thiol–thione tautomer DMcT 2 (Fig. 1) was found to be the most stable form in the gas phase with ΔE_{elec} to the thione DMcT 1 of 24.6 kJ mol⁻¹ and thiol DMcT 5 of 42.7 kJ mol⁻¹. All the values are displayed in Table 1. The fact that the mixed thiol–thione tautomer was predicted to be the most stable form is in accordance with X-ray investigations⁸ of the bulk phase and with an early *ab initio* study⁹ of the gas-phase equilibria at the STO-3G and 4-31G* levels.

IR spectrum of matrix-isolated McMT

An FT-IR spectrum of McMT isolated in an Ar matrix is presented in Fig. 2. Vibrational data and assignments are given in Table 2. The vibrational activity of McMT can be deduced from the molecular point group C_s , and the resulting 27 fundamental vibrations, of which all bands are both Raman and IR active, may be represented as

$$\Gamma_{\text{vib}} = 18 A' + 9 A'' \quad (1)$$

All the intense bands have their well predicted counterparts in the spectrum calculated for McMT 1 at the B3LYP/6-311+G(d,p) level (spectrum B in Fig. 2). Calculated spectra

Table 2 Vibrational data ν_{obs} (cm^{-1}) and assignments for matrix-isolated and bulk McMT. Calculated harmonic frequencies ν_{calc} (cm^{-1} , unscaled), IR intensities (km mol^{-1}) and fit factors (ratio $\nu_{\text{obs,matrix}}/\nu_{\text{calc}}$) for McMT 1 [B3LYP/6-311+G(d,p)]

ν_{obs}	Matrix-isolated McMT (FT-IR) ^a	Bulk McMT (FT-Raman)	ν_{calc} McMT 1	Assignment
3449 s		3051	3623 (83, 0.95)	$\nu(\text{NH}) A'$
2982 vw		2963	3131 (3, 0.95)	$\nu_{\text{as}}(\text{CH}_3) A'$
2937 vw		2914	3092 (6, 0.95)	$\nu_{\text{as}}(\text{CH}_3) A''$
2829 vw		2870	3037 (14, 0.93)	$\nu_s(\text{CH}_3) A'$
—		1553	1620 (15)	$\nu(\text{C}=\text{N}) A'$
1440 m			1480 (20, 0.97)	$\delta_{\text{as}}(\text{CH}_3) A'$
1430 vw		1451	1475 (13, 0.97)	$\delta_{\text{as}}(\text{CH}_3) A''$
1421 vs			1462 (211, 0.97)	$\delta(\text{NH}) A'$
1381 w		1378	1416 (11, 0.98)	$\delta_s(\text{CH}_3) A'$
1240 vs		1271	1260 (247, 0.98)	$\nu(\text{CN}) A'$
1229 w		1197	1208 (7, 1.02)	$\nu(\text{CC}) A'$
1138 m		1136	1148 (38, 0.99)	$\nu(\text{NN}) A'$
1079 s		1080	1071 (116, 1.01)	$\nu(\text{S}=\text{C}-\text{N}) A'$
1061 vw			1057 (0.5, 1.00)	$\delta(\text{CH}_3)_{\text{rock}} A''$
966 w		977	986 (16, 0.98)	$\delta(\text{CH}_3)_{\text{rock}} A'$
738 m		744	739 (32, 1.00)	$\delta(\text{ring}) A'$
		660	647 (1)	$\nu_s(\text{C}-\text{S}) A'$
615 m		627	603 (31, 1.02)	$\nu_{\text{as}}(\text{C}-\text{S}) A'$
589 m		588	600 (46, 0.98)	$\delta(\text{NH}) A''$
553 m			549 (23, 1.01)	$\delta(\text{ring}/\text{NH}) A'$
518 m			526 (17, 0.99)	$\delta(\text{ring}/\text{NH}) A''$
433 w		432	436 (6, 0.99)	$\delta(\text{ring}) A'$
		346	346 (2)	$\delta_{\text{as}}(\text{S}=\text{C}-\text{S}/\text{CCH}_3) A'$
		256	316 (1)	$\delta(\text{ring}) A''$
		235	230 (0.03)	$\delta_s(\text{S}=\text{C}-\text{S}/\text{CCH}_3) A'$
		153	126 (0.07)	$\tau(\text{CH}_3) A''$
		104	109 (0.05)	$\delta(\text{ring}) A''$
		86		Lattice mode
		66		Lattice mode

^a Unassigned IR band at 1125 cm^{-1} . The designations of the normal modes give only a rough description of the motion, which is particularly true for the low-energy modes.

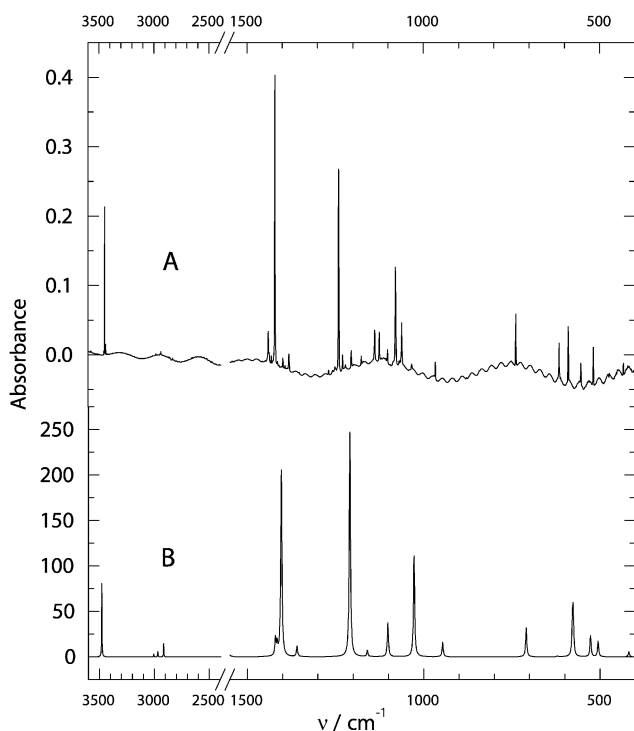


Fig. 2 The experimental (A) and calculated (B) infrared spectra of 2-mercapto-5-methyl-1,3,4-thiadiazole, McMT: (A) isolated in an Ar matrix, (B) calculated for McMT 1 at the B3LYP/6-311+G(d,p) level (scaling factor 0.96). For assignments see Table 2.

for McMT 2 and McMT 3 are included in the ESI. The observed spectrum can be explained if the tautomeric equilibrium strongly favours tautomer McMT 1, as the strong absorption at 3449 cm^{-1} can be assigned to the $\nu(\text{NH})$ stretch-

ing mode and no $\nu(\text{SH})$ modes are observed. However, because the absorption due to $\nu(\text{SH})$ is generally quite weak, it is possible that minor amounts of a thiol species may be overlooked at first glance, if we assume a mixture of isomers. We can circumvent this limitation by taking into account other characteristic vibrational modes which are more intense, e.g. the SH bending mode. The in-plane $\delta(\text{SH})$ is predicted to occur with medium intensity at 911 and 933 cm^{-1} for McMT 2 and McMT 3, respectively. In this range, only $\delta(\text{CH}_3)_{\text{rock}}$ is expected for all McMT isomers and $\delta(\text{SH})$ for McMT 2 and McMT 3. In fact only one band at 966 cm^{-1} is observed in the experimental spectrum and is attributed to the $\delta(\text{CH}_3)_{\text{rock}}$ of McMT 1 (*cf.* Table 2). The two $\nu(\text{CH}_3)$ antisymmetric and one $\nu(\text{CH}_3)$ symmetric stretching modes of the exocyclic methyl moiety at 2982 , 2937 , and 2829 cm^{-1} appear relatively weak. The most intense absorption at 1421 cm^{-1} can be attributed to the thioamide $\delta(\text{NH})$ in-plane deformation; weaker absorptions at 1440 and 1381 cm^{-1} are ascribed to antisymmetric and symmetric CH_3 bending modes. The intense $\nu(\text{C}=\text{N})$ stretching mode appears at 1240 cm^{-1} . The IR band at 1079 cm^{-1} can be ascribed to ring deformations associated with in-plane vibrations of the NCS-moiety (thioamide band). Altogether, the spectrum of the matrix-isolated species as well as that of the bulk phase (*cf.* Table 2) agrees fully with the structure McMT 1 given in Scheme 1. Comparison of the data of the matrix-isolated species with those of the bulk phase shows that there is a shift of about 400 cm^{-1} for the $\nu(\text{NH})$ stretching mode, caused by intermolecular interactions like hydrogen bonding in the solid state.

IR spectrum of matrix-isolated DMcT

The survey spectrum of DMcT isolated in an Ar matrix is shown in Fig. 3, vibrational data and assignments are listed in Table 3. In the case of DMcT isomers 1, 4 and 5 with C_{2v}

Table 3 Vibrational data ν_{obs} (cm^{-1}) and assignments for matrix-isolated and bulk DMcT. Calculated harmonic frequencies ν_{calc} (cm^{-1} , unscaled), IR intensities (km mol^{-1}) and fit factors (ratio $\nu_{\text{obs,matrix}}/\nu_{\text{calc}}$) for thione–thiol tautomer DMcT 2 [B3LYP/6-311+G(d,p)]^a

ν_{obs}		ν_{calc}	Assignment
Matrix-isolated DMcT (FT-IR)	Bulk DMcT (FT-Raman)	DMcT 2	
3574 w	2848		^b
3445 s	3052	3623 (89, 0.95)	$\nu(\text{NH}) \text{ A}'$
2591 w	2482	2660 (2, 0.97)	$\nu(\text{SH}) \text{ A}'$
1507 m	1510	1556 (70, 0.97)	$\nu(\text{C}=\text{N})/\delta(\text{NH}) \text{ A}'$
1416 vs	1452	1461 (212, 0.97)	$\delta(\text{NH}) \text{ A}'$
1232 vs	1282	1255 (272, 0.98)	$\nu(\text{C}-\text{N}) \text{ A}'$
1131 s	1113	1136 (41, 1.00)	$\nu(\text{NN}) \text{ A}'$
1065 m	1079	1077 (103, 0.99)	$\nu(\text{C}-\text{S})/\delta(\text{SH}) \text{ A}'$
1052 m	1041	1063 (65, 0.99)	$\nu_{\text{as}}(\text{S}=\text{C}-\text{S}) \text{ A}'$
892 w	941	901 (35, 0.99)	$\delta(\text{SH}) \text{ A}'$
701 m	714	690 (68, 1.02)	$\nu_{\text{as}}(\text{C}-\text{S}-\text{C}) \text{ A}'$
640 w	658	634 (23, 1.01)	$\nu_{\text{s}}(\text{C}-\text{S}-\text{C}) \text{ A}'$
572 m		577 (38, 0.99)	$\delta(\text{NH}) \text{ A}''$
544 w	534	533 (2, 1.02)	$\delta(\text{HS}-\text{CS}-\text{C}) \text{ A}'$
544 w	534	529 (12, 1.03)	$\delta(\text{ring}/\text{NH}) \text{ A}''$
515 m	482	524 (33, 0.98)	$\delta(\text{ring}/\text{NH}) \text{ A}''$
	372	372 (3)	$\delta(\text{C}-\text{S}-\text{C}) \text{ A}'$
	313	312 (2)	$\delta_{\text{as}}(\text{S}=\text{C}-\text{N}/\text{HS}-\text{C}-\text{N}) \text{ A}'$
	313	296 (0.1)	$\delta(\text{ring}) \text{ A}''$
	203	189 (1)	$\delta_{\text{s}}(\text{S}=\text{C}-\text{N}/\text{HS}-\text{C}-\text{N}) \text{ A}'$
	117	171 (23)	$\delta(\text{SH}) \text{ A}''$
	96	93 (0.4)	$\delta(\text{ring}) \text{ A}''$
	72		Lattice mode

^a Unassigned weak IR bands at 1361 and 1085 cm^{-1} . The designations of the normal modes give only a rough description of the motion, which is particularly true for the low-energy modes. ^b Overtone or combination band.

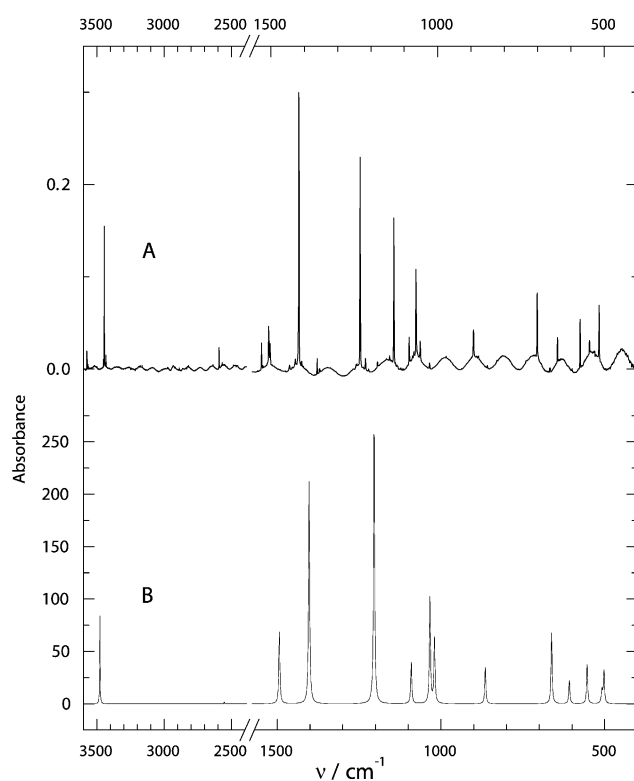


Fig. 3 The experimental (A) and calculated (B) infrared spectra of 2,5-dimercapto-1,3,4-thiadiazole, DMcT: (A) isolated in an Ar matrix, (B) calculated for DMcT 2 at the B3LYP/6-311+G(d,p) level (scaling factor 0.96). For assignments see Table 3.

symmetry (Scheme 2), we expect 21 fundamental vibrations which can be expressed as

$$\Gamma_{\text{vib}} = 8 \text{ A}_1 + 3 \text{ A}_2 + 7 \text{ B}_1 + 3 \text{ B}_2 \quad (2)$$

of which all are Raman active and the 3 A_2 modes are IR inactive. In the case of DMcT isomers 2, 3 and 6 with C_s

symmetry (Scheme 2), the resulting 21 fundamental vibrations, of which all modes are Raman and IR active, transform according to

$$\Gamma_{\text{vib}} = 15 \text{ A}' + 6 \text{ A}'' \quad (3)$$

The observed spectrum can be explained if the tautomeric equilibrium strongly favours tautomer DMcT 2, because the intense $\nu(\text{N}-\text{H})$ as well as the weaker $\nu(\text{S}-\text{H})$ stretching modes are observed at 3445 and 2591 cm^{-1} , respectively. In Fig. 3 the experimental spectrum (A) can be compared directly with the calculated IR spectrum (B) for isomer DMcT 2. Calculated spectra for the other DMcT isomers are included in the ESI. As in the case of McMT, the most intense absorptions are caused by thioamide vibrations. The $\delta(\text{NH})$ in-plane mode appears at 1416 cm^{-1} . A weaker but related absorption at 1507 cm^{-1} can be attributed to a combination of the $\delta(\text{NH})$ deformation and the $\nu(\text{C}=\text{N})$ stretching mode, whereas the intense $\nu(\text{C}=\text{N})$ stretching mode appears at 1232 cm^{-1} . The vibration at 1131 cm^{-1} is ascribed to $\nu(\text{NN})$, weaker absorptions at 1065 and 1052 cm^{-1} are assigned to $\nu(\text{C}-\text{S})$ and $\nu_{\text{as}}(\text{S}=\text{C}-\text{S})$. The in-plane $\delta(\text{SH})$ mode appears at 892 cm^{-1} , and the stretching modes of the cyclic $\text{C}-\text{S}$ bonds appear at 701 and 640 cm^{-1} . Other absorptions of weaker intensity at 572, 544, and 515 cm^{-1} are caused by out-of-plane $\delta(\text{NH})$ and ring deformations.

As seen in the case of McMT, when comparing the IR data of the matrix-isolated species with the Raman spectrum of the bulk phase, one also notes a shift of about 400 cm^{-1} for the $\nu(\text{N}-\text{H})$ stretching mode of DMcT, which can be explained by intermolecular interactions like hydrogen bonding in the solid state. The $\nu(\text{S}-\text{H})$ stretching vibration is also shifted by 110 cm^{-1} . Contrary to the observations of Edwards *et al.*,¹⁴ we were able to observe $\nu(\text{N}-\text{H})$ and $\nu(\text{S}-\text{H})$ stretching modes in the IR spectrum of matrix-isolated DMcT as well as in the Raman spectrum of bulk DMcT. These experimental results give proof of the predominant existence of thiol–thione tautomer DMcT 2, in accordance with earlier X-ray investigations⁸ and with our DFT studies (see above), whereas Edwards *et al.*¹⁴ favoured the thiol–thiol tautomer DMcT 4.

Thermolyses of thiadiazoles

We have investigated the high-vacuum thermolysis of 2,5-dimercapto-1,3,4-thiadiazole (DMcT) and 2-mercapto-5-methyl-1,3,4-thiadiazole (McMT) with matrix-isolation techniques. A continuous gas flow of a thiadiazole–argon mixture was passed through a thermolysis oven and immediately thereafter trapped on a cooled matrix window to ensure that a maximum of volatile fragments emerging from the oven was trapped. In order to characterise a pure thiadiazole–argon matrix without any fragmentation products present, we have conducted experiments at oven temperatures from ambient to 120 °C. The spectra obtained were compared with calculated harmonic frequencies and with data from the bulk phase (see Raman data of McMT and DMcT in Tables 2 and 3). Having succeeded in getting a spectrum of the starting material, the oven temperature was slowly increased to bring about thermolysis.

Thermolysis of McMT. Selected IR spectra of matrix-isolated product mixtures obtained at different thermolysis temperatures are given in Fig. 4. At temperatures up to 200 °C

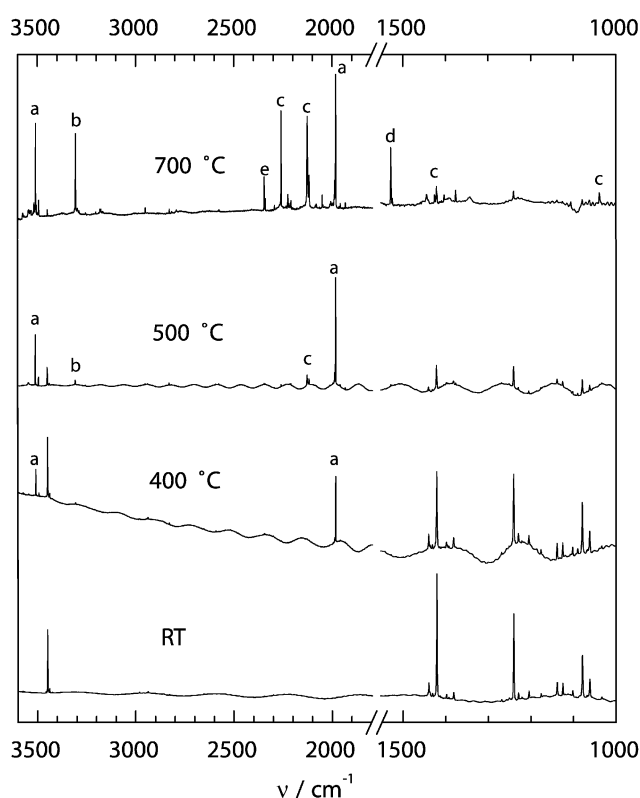


Fig. 4 Spectra of matrix-isolated products of McMT from different thermolyses, trapped in argon at 20 K. (a) HNCS, (b) HCN, (c) CH₃NCS, (d) CS₂, (e) contaminant CO₂. Wavenumbers are given in the text.

no reaction was observed. At 200 °C the first decomposition product bands were detected. The most intense product band appears at 1982 cm⁻¹ and can be attributed to the $\nu(\text{NC})$ of isothiocyanic acid HNCS.¹⁵ In the N–H stretching region a second signal appears above the 3449 cm⁻¹ stretching mode of McMT at 3509 cm⁻¹, which is ascribed to the $\nu(\text{NH})$ mode of HNCS. Other measured frequencies at 987 [$\nu(\text{CS})$], 578 [$\gamma(\text{NCS})$], and 468 cm⁻¹ [$\delta(\text{NCS})$] are in good agreement with published data for this well-known molecule,¹⁵ so that HNCS can unequivocally be identified as the first decomposition product (a in Fig. 4). With increasing temperatures, the IR bands of the starting material decrease in intensity and, in addition to those due to HNCS, other new bands appear. The most interesting spectral region is the one around 2100 cm⁻¹,

where a doublet at 2126 and 2117 cm⁻¹ grows in. This doublet is characteristic of the $\nu_{\text{as}}(\text{NCS})$ mode of methyl isothiocyanate, CH₃NCS (c in Fig. 4).¹⁶ The signal at 1038 cm⁻¹ can be assigned to the symmetric stretch. The NCS asymmetric stretch of methyl isothiocyanate is known to shift from 2089 cm⁻¹ in the gas phase to a doublet at 2126 and 2118 cm⁻¹ in argon matrices but to a single band at 2135 cm⁻¹ in nitrogen matrices.¹⁶ At 1421 cm⁻¹ the deformation vibration of the methyl group occurs, and at 2259 cm⁻¹ an overtone of the symmetric stretch in Fermi resonance with the asymmetric stretching modes around 2126 cm⁻¹ can be observed in agreement with reported data.¹⁶ Other vibrational modes of CH₃NCS are too weak to be detected under our reaction conditions. Another product, HCN, can also be detected with its vibrations appearing at 3306 and 721 cm⁻¹ (b in Fig. 4). A relatively strong absorption at 1528 cm⁻¹ cannot be explained by the thermolysis products accounted for so far, but can be attributed tentatively to a stretching mode of CS₂ (d in Fig. 4). A set of frequencies at 1529 cm⁻¹ for the stretching mode, and at 397 and 395 cm⁻¹ for the bending mode of CS₂ in argon matrices have been reported,¹⁷ but unfortunately the bands due to the bending mode were below our detection limit (400 cm⁻¹).

In summary, as shown in Scheme 3, the decomposition products of McMT are HNCS, CH₃NCS, HCN, and presumably CS₂. Other possible products, e.g. acetonitrile or hydrogen sulfide, were clearly excluded by comparing experimental data with vibrational data taken from the literature or from DFT calculations. In contrast to McMT, decomposition of a related 5-methyl-1,3,4-oxathiazol-2-one was shown to produce acetonitrile among other products.¹⁸ In the case of McMT the fragmentation can be rationalised by assuming a cleavage of the heterocycle between the N–N and C–S bonds. This would result in the formation of isothiocyanic acid, HNCS, and an intermediate nitrene which would rapidly undergo an intramolecular insertion reaction to give methyl isothiocyanate, CH₃NCS. However, the product ratio between HNCS and CH₃NCS depends on the thermolysis temperature. At 400 °C no CH₃NCS bands are visible although all the vibrational modes of HNCS can be seen. At 500 °C a weak doublet at 2126 and 2117 cm⁻¹ [$\nu_{\text{as}}(\text{NCS})$] indicates small amounts of CH₃NCS, but at 700 °C the relative amount of CH₃NCS with respect to HNCS is strongly increased. Several effects might be responsible for this observation. First, HNCS exhibits very strong IR absorptions and even traces of HNCS can be detected. Second, the proposed nitrene precursor to CH₃NCS might react effectively with the oven surface over a certain temperature range and remain adsorbed at the lower temperature. Third, the amount of HNCS could be reduced at higher temperatures if we assume that a fraction of these molecules loses atomic sulfur to form HNC, which then rearranges to the thermodynamically more stable HCN. As it can be seen in Fig. 4, the amount of HCN increases with increasing temperature. Of course, matrix-isolation techniques allow the reaction products to be identified, but not the precise decomposition mechanisms, which must therefore remain somewhat speculative.

Thermolysis of DMcT. In Fig. 5 selected IR spectra of matrix-isolated product mixtures from different thermolysis temperatures are given. When the oven temperature was below 140 °C no reaction was observed and only intact DMcT was trapped onto the matrix window. At 140 °C a weak signal at 1982 cm⁻¹ appeared which, as discussed for McMT, can be attributed to the $\nu(\text{NC})$ stretching mode of isothiocyanic acid HNCS. At higher temperatures a higher yield of HNCS is reached so that the weaker modes of this molecule become detectable {3509 [$\nu(\text{NH})$], 987 [$\nu(\text{CS})$], 578 [$\gamma(\text{NCS})$], and 465 cm⁻¹ [$\delta(\text{NCS})$], a in Fig. 5}. Additionally, a weak signal at 3544 cm⁻¹ may be caused by an HNCS dimer according to Durig and Wertz.¹⁵ The vibrational frequencies of HNCS are identical to the data found in the case of the McMT thermolysis with the

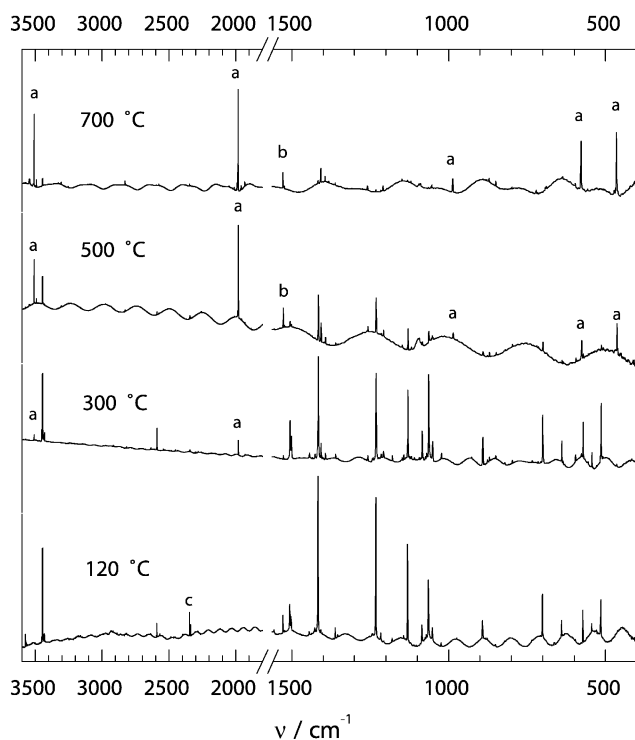
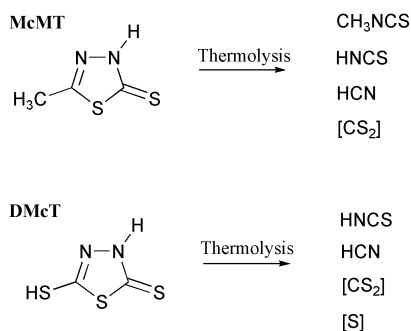


Fig. 5 Spectra of the thermolysis products of DMcT at different temperatures up to 700 °C, trapped in argon at 20 K. (a) HNCS, (b) CS₂, (c) contaminant CO₂.

exception of the $\delta(\text{NCS})$ mode observed at 465 cm⁻¹ (468 cm⁻¹ in the case of McMT). HCN can also be detected with its vibrations appearing at 3306 and 721 cm⁻¹. An absorption at 1528 cm⁻¹, visible at temperatures higher than 300 °C, may be attributed tentatively to a stretching mode of CS₂ as seen for the McMT thermolysis (b in Fig. 5).



Scheme 3

For the thermolysis of DMcT a fragmentation can be assumed involving a cleavage of the heterocycle between the N=N and C-S bonds (Scheme 3). This would result in the formation of isothiocyanic acid, HNCS, thiocyanic acid, HSCN (which will rapidly undergo a thermodynamically driven reaction to the more stable isomer HNCS), and presumably atomic sulfur, which could not be detected by techniques available in our current study. Diazirines, which are known to be formed upon electron ionisation of DMcT,⁴ are not involved in the fragmentation processes initiated by thermolyses.

Conclusions

Mercapto-functionalised thiadiazoles and derivatives, which have been widely studied for analytical and industrial applications and linked to processes in which high temperatures occur, were subjected to thermolysis, and vibrational spectroscopic studies were performed to illuminate the thermolysis behaviour of these compounds. High-vacuum thermolysis

experiments with 2,5-dimercapto-1,3,4-thiadiazole and 2-mercapto-5-methyl-1,3,4-thiadiazole were performed between ambient temperature and 800 °C. The thermolysis products were trapped by matrix-isolation techniques and characterised by IR spectroscopy. Thermolysis of 2,5-dimercapto-1,3,4-thiadiazole gives HNCS, CS₂ and HCN, whereas 2-mercapto-5-methyl-1,3,4-thiadiazole shows a more complex fragmentation pattern forming HNCS, CH₃NCS, HCN and CS₂. These results may give some useful information for some technical applications, as the observed products may play a role in secondary chemical reactions with other materials.

Furthermore, the tautomeric equilibrium of mercaptothiadiazoles has been a point of controversy for many authors. We have studied the tautomeric equilibria and structures of 2,5-dimercapto-1,3,4-thiadiazole and 2-mercapto-5-methyl-1,3,4-thiadiazole with *ab initio* and DFT computations and found the thione-thiol and the thione tautomer, respectively, to be the most stable. The predictions were corroborated experimentally by vibrational spectroscopy and X-ray crystallography. The theoretically favoured thione tautomer of McMT was shown to occur not only in cryogenic argon matrices, where the molecules are isolated and no hydrogen bonding was observed in the IR spectra, but also in the solid state, where an additional stabilising effect of N-H...S hydrogen bonding can be considered. In fact, it has been shown that 2-mercapto-5-methyl-1,3,4-thiadiazole, in contrast to related compounds, forms chains *via* N-H...S hydrogen bonds (N...S distance 328.3 pm).¹²

Acknowledgements

Thanks are due to Sabine Bendix and Gerd Bollmann for their support and to Professor Christof Wöll and Stefanie Gil Girol for the beneficial collaboration on the surface chemistry of the thiadiazoles. We would like to thank the Deutsche Forschungsgemeinschaft (DFG) and the Fonds der Chemischen Industrie (FCI) for financial support.

References

- G. Kornis, *1,3,4-Thiadiazoles. Comprehensive Heterocyclic Chemistry*, A. R. Katritzky and C. W. Rees, Eds., Pergamon Press, Oxford, 1984, vol. 6, part 4B, p 545.
- E. Shouji and D. A. Buttry, *J. Phys. Chem. B*, 1998, **102**, 1444.
- F. Hipler, S. Gil Girol, R. A. Fischer and Ch. Wöll, *Materialwiss. Werkstofftech.*, 2000, **31**, 872.
- F. Bottino, S. Caccamese and S. Pappalardo, *Org. Mass Spectrom.*, 1982, **17**, 335.
- G. I. Yranzo, J. Elguero, R. Flammang and C. Wentrup, *Eur. J. Org. Chem.*, 2001, 2209.
- R. Flammang, P. Gerbaux, E. H. Mørkved, M. W. Wong and C. Wentrup, *J. Phys. Chem.*, 1996, **100**, 17452.
- A. R. Katritzky, J. Borowiecka, W.-Q. Fan and L. H. Brannigan, *J. Heterocycl. Chem.*, 1991, **28**, 1139; A. R. Katritzky, Z. Wang and R. J. Offerman, *J. Heterocycl. Chem.*, 1990, **27**, 139.
- J. W. Bats, *Acta Crystallogr., Sect. B: Struct. Crystallogr. Cryst. Chem.*, 1976, **32**, 2866.
- S. Millefiori and A. Millefiori, *J. Mol. Struct.*, 1987, **151**, 373.
- J. H. Looker, N. A. Khatri, R. B. Patterson and C. A. Kingsbury, *J. Heterocycl. Chem.*, 1978, **15**, 1383.
- M. J. Frisch, G. W. Trucks, H. B. Schlegel, G. E. Scuseria, M. A. Robb, J. R. Cheeseman, V. G. Zakrzewski, J. A. Montgomery, R. E. Stratmann, J. C. Burant, S. Dapprich, J. M. Millam, A. D. Daniels, K. N. Kudin, M. C. Strain, O. Farkas, J. Tomasi, V. Barone, M. Cossi, R. Cammi, B. Mennucci, C. Pomelli, C. Adamo, S. Clifford, J. Ochterski, G. A. Petersson, P. Y. Ayala, Q. Cui, K. Morokuma, D. K. Malick, A. D. Rabuck, K. Raghavachari, J. B. Foresman, J. Cioslowski, J. V. Ortiz, B. B. Stefanov, G. Liu, A. Liashenko, P. Piskorz, I. Komaromi, R. Gomperts, R. L. Martin, D. J. Fox, T. Keith, M. A. Al-Laham, C. Y. Peng, A. Nanayakkara, C. Gonzalez, M. Challacombe, P. M. W. Gill, B. G. Johnson, W. Chen, M. W. Wong, J. L. Andres, M. Head-Gordon, E. S. Replogle and J. A. Pople, GAUSSIAN 98, Gaussian Inc., Pittsburgh, PA, 1998.

- 12 F. Hipler, M. Winter and R. A. Fischer, unpublished work.
- 13 The experimental N–H bond length differs considerably from the theoretical figure, but as the H-atom position is not clear in the X-ray experiment and hydrogen-bonding has not been taken into account, the comparison is somewhat meaningless.
- 14 H. G. M. Edwards, A. F. Johnson and E. E. Lawson, *J. Mol. Struct.*, 1995, **351**, 51.
- 15 J. R. Durig and D. W. Wertz, *J. Chem. Phys.*, 1967, **46**, 3069. Known vibrational modes of matrix-isolated HNCS are found at 3505, 1979, 988, 577, and 461 cm^{-1} .
- 16 J. R. Durig, J. F. Sullivan, D. T. Durig and S. Cradock, *Can. J. Chem.*, 1985, **63**, 2000.
- 17 A. Givan, A. Loewenschuss, K. D. Bier and H. J. Jodl, *Chem. Phys.*, 1986, **106**, 151.
- 18 T. Pasinszki, T. Kárpáti and N. P. C. Westwood, *J. Phys. Chem. A*, 2001, **105**, 6258.